

INFLUENCE OF TITANIUM TETRAISOPROPOXIDE: ACETYLACETONE MOLAR RATIO ON THE GAS SENSING PERFORMANCE OF TiO₂ THIN FILMS DEPOSITED VIA SPRAY PYROLYSIS**Mandakini Chaudhari¹, Rajendrakumar Ahirrao^{2*}, Astha Sing³ and Avinash Agrawal⁴**¹Research Scholar and ³Research Guide, Department of Physics, Shri JIT University Jhunjhunu, Rajasthan, India²Research Co-Guide, Department of Physics, Uttamrao Patil College, Dahiwel, Dhule Maharashtra, India⁴Department of Physics, Bareilly College, Bareilly (U. P.) India²ahirraorb@gmail.com**ABSTRACT**

Titanium dioxide (TiO₂) thin films were synthesized using spray pyrolysis with titanium tetraisopropoxide (TTIP) and acetylacetonone (AcAc) in molar ratios of 1:2 and 1:3 to study how precursor composition affects their structural, optical, electrical, and gas sensing properties. X-ray diffraction (XRD) analysis revealed that both ratios produced phase-pure anatase TiO₂. Increasing the AcAc ratio from 1:2 to 1:3 resulted in smaller crystallite sizes (~17.8 nm to ~14.2 nm), higher lattice strain, and increased dislocation density. Scanning electron microscopy (SEM) and energy dispersive X-ray spectroscopy (EDS) revealed that the 1:2 films were more uniform and densely packed, while the 1:3 films had higher porosity and oxygen-rich surfaces. Raman and X-ray photoelectron spectroscopy (XPS) confirmed the presence of oxygen vacancies and changes in hydroxyl groups, which improved gas sensing behavior. Electrical measurements indicated that the 1:3 films had higher activation energy and lower mobility compared to the 1:2 films. Gas sensing tests showed that the 1:3 films exhibited enhanced sensitivity, as well as faster response and recovery times, particularly for hydrogen (H₂) at 300°C, attributed to their higher surface reactivity and defect concentration. These findings emphasize the importance of precursor engineering in optimizing TiO₂ thin films for high-performance gas sensors.

1. INTRODUCTION

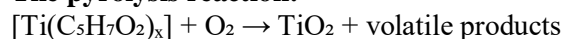
Titanium dioxide (TiO₂) thin films are promising for gas sensing due to their stability, tunable electronic properties, and sensitivity to gases like VOCs, NO_x, and CO [1–3]. Their performance depends critically on crystallographic phase, morphology, and defect chemistry, which are governed by synthesis parameters [4,5]. Spray pyrolysis offers a scalable route to tailor these properties via precursor engineering [6,7]. Titanium tetraisopropoxide (TTIP) is a common precursor but requires acetylacetonone (AcAc) as a stabilizer to control hydrolysis [8,9]. While the TTIP:AcAc ratio influences film properties [10], its impact on gas sensing remains understudied. This work systematically evaluates 1:2 and 1:3 TTIP:AcAc ratios, linking structural (XRD, SEM, TEM), chemical (XPS, Raman), and gas-sensing properties. The results demonstrate how precursor tuning optimizes TiO₂ films for high-performance sensors.

2. EXPERIMENTAL**2.1. Precursors**

TTIP (≥97%, Otto Chemie) was used as the titanium source due to its high reactivity, with AcAc (≥99%, LOBA Chemie) added as a stabilizer to control hydrolysis kinetics [13-15]. Ethanol (≥99%, LOBA Chemie) served as the solvent. This stabilization approach aligns with previous studies on metal oxide films [16,17].

2.2 Synthesis of TiO₂ Thin Films

TiO₂ films were prepared via spray pyrolysis using TTIP:AcAc molar ratios of 1:2 and 1:3. For each ratio, 1 mmol TTIP was dissolved in 20 mL ethanol, followed by dropwise addition of 2 or 3 mmol AcAc. After 30 min stirring, the 10 mM solution was diluted with water and sprayed onto glass substrates at 300°C.

The pyrolysis reaction:

yielded films for gas-sensing characterization [18-20].

2.2.1 TiO₂ Thin Film Deposition

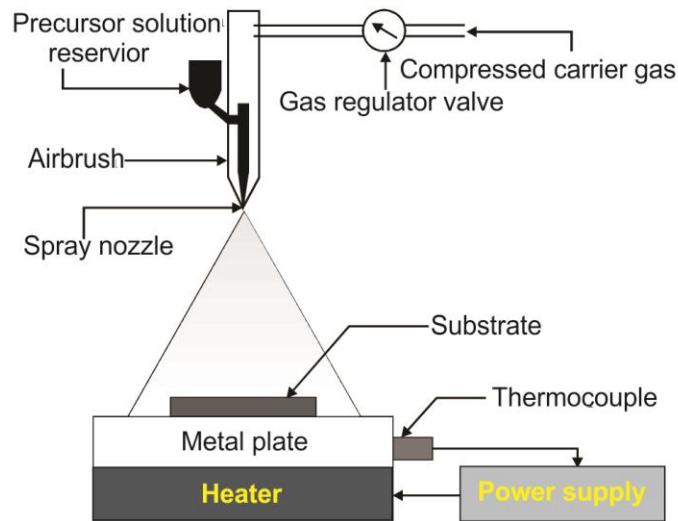


Fig. 1. Schematic diagram of spray pyrolysis system.

TiO₂ thin films were deposited on borosilicate glass substrates via spray pyrolysis using 0.1 M TTIP solutions with TTIP:AcAc molar ratios of 1:2 and 1:3. For each ratio, 3.5 mL of TTIP was combined with the appropriate amount of AcAc, diluted to 60 mL with ethanol, and stirred for 1 hour to ensure homogeneity. The resulting solutions were then sprayed onto heated substrates at 350°C using compressed air (10 L/min flow rate) as the carrier gas. Finally, the deposited films were annealed at 500°C for 1 hour in air to enhance crystallinity [21].

3. RESULTS AND DISCUSSION

3.1. XRD of Thin films of 1:2 and 1:3 Molar Ratio.

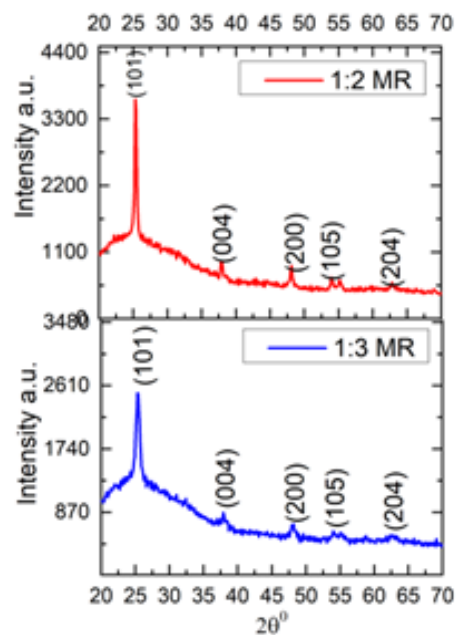


Fig.2.X ray diffraction Study of TTIP:AcAc

The XRD analysis confirmed the formation of pure anatase phase TiO₂ (JCPDS 21-1272) for both 1:2 and 1:3 molar ratio films, with characteristic diffraction peaks observed at 25.3° (101), 37.8° (004), 48.0° (200), 54.0° (105), and 63.0° (204) (Fig. 2). The 1:2 MR films exhibited sharper (101) peaks (FWHM ~0.008 rad) corresponding to larger crystallite size (17.8 nm) and lower defect density ($3.15 \times 10^{-3} \text{ nm}^{-2}$), indicating superior crystallinity. In contrast, the 1:3 MR films showed broader peaks (FWHM ~0.010 rad) with smaller crystallites (14.2 nm) and higher defect concentration ($4.96 \times 10^{-3} \text{ nm}^{-2}$). Both films maintained identical tetragonal lattice parameters ($a=b=0.378 \text{ nm}$, $c=0.951 \text{ nm}$), confirming structural stability across molar ratios. The 1:3 MR films' reduced crystallite size and increased defect density enhance gas sensing performance through three key mechanisms: (1) greater surface-to-volume ratio for gas adsorption, (2) more active surface sites, and (3) oxygen vacancy-mediated charge transfer [26,27]. While the 1:2 MR films demonstrate better crystallinity suitable for optoelectronic applications, the defect-rich structure of 1:3 MR films proves particularly advantageous for gas sensing applications [28]. (Structural parameters are summarized in Table 1.)

Table 1: Comprehensive Structural Comparison

Parameter	1:2 MR Sample	1:3 MR Sample
Dominant Phase	Anatase TiO ₂	Anatase TiO ₂
Crystal Structure	Tetragonal	Tetragonal
Strongest Peak (2θ)	25.3° (101)	25.3° (101)
Crystallite Size (D)	~17.8 nm	~14.2 nm
FWHM (β)	~0.008 rad	~0.010 rad
Dislocation Density (δ)	$3.15 \times 10^{-3} \text{ nm}^{-2}$	$4.96 \times 10^{-3} \text{ nm}^{-2}$
Lattice Parameter a	~0.378 nm	~0.378 nm
Lattice Parameter b	~0.378 nm (<i>same as a</i>)	~0.378 nm (<i>same as a</i>)
Lattice Parameter c	~0.951 nm	~0.951 nm
Peak Sharpness	Sharper (better crystallinity)	Broader (more defects)
Phase Purity	High (no extra peaks)	High (no extra peaks)

3.2. Scanning Electron Microscope (SEM) and Elemental analysis (EDS)

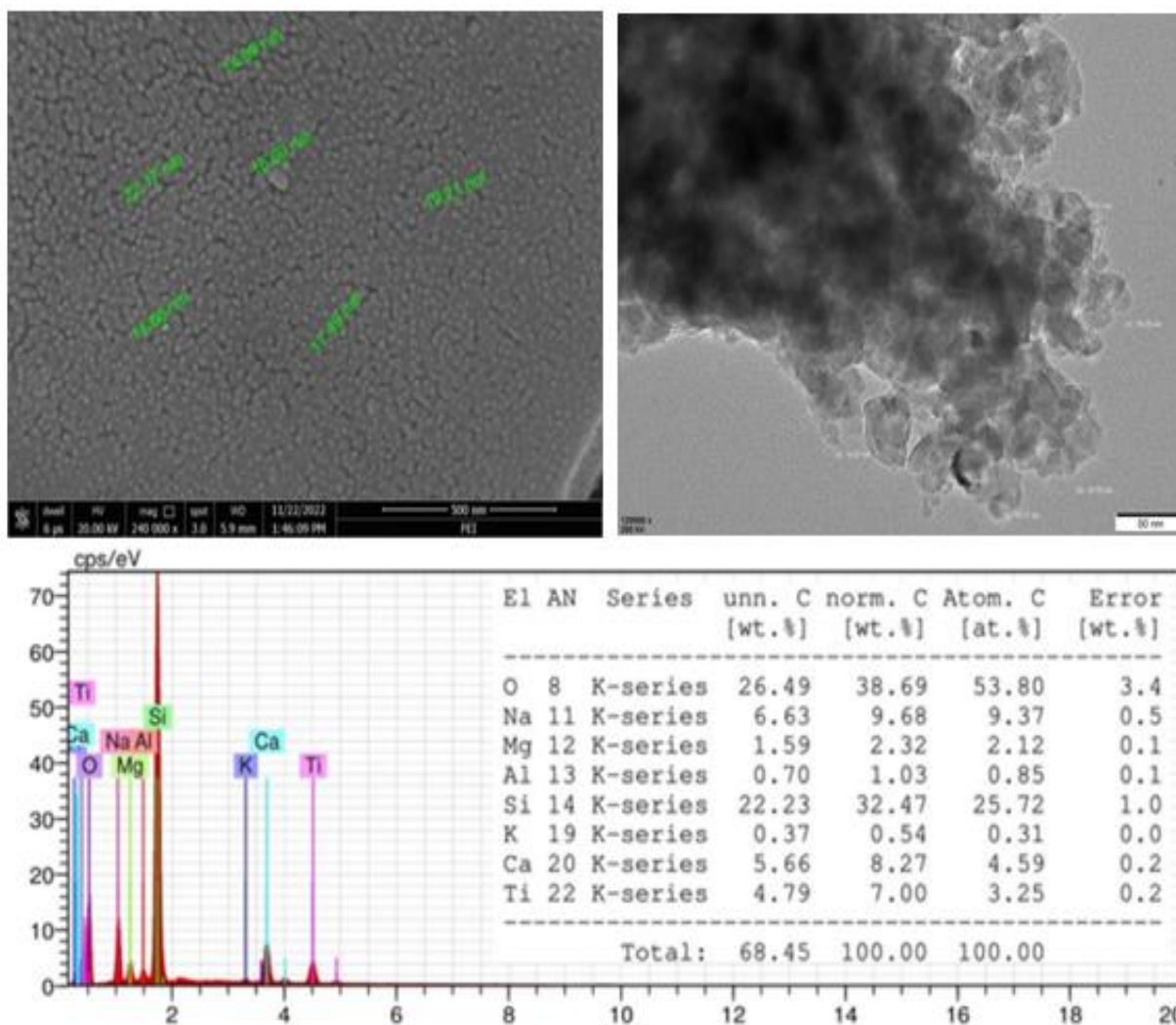


Fig. 3. EDX spectra and microstructure analysis tables of TiO₂ thin films synthesized using TTIP and AcAc precursors with 1:2 molar ratio annealed at 500°C for 30 minutes.

The TiO₂ thin films synthesized using titanium isopropoxide (TTIP) and acetylacetonate (AcAc) at molar ratios of 1:2 and 1:3 exhibit distinct structural and compositional properties that influence their gas sensing performance.

For the 1:2 molar ratio sample (Fig. 3), SEM images reveal a uniform and densely packed nanostructure with grain sizes ranging between ~12–27 nm, which enhances the surface-to-volume ratio and electron mobility—key factors for efficient gas sensing [29]. TEM analysis further confirms a semi-crystalline network with interconnected grains, facilitating gas adsorption and charge transfer. The EDX data indicates an oxygen content of 38.69 wt.% (53.80 at.%), slightly exceeding the stoichiometric TiO₂ ratio (O:Ti ≈ 2.1:1). This suggests the presence of oxygen-rich surface states or interstitial oxygen, which may enhance surface redox reactions beneficial for gas sensing [30]. The titanium content is measured at 7.00 wt.% (3.25 at.%), consistent with TiO₂ stoichiometry. Minor impurities such as Na, Ca, and Mg likely originate from substrate or precursor residues and may influence defect chemistry without significantly impairing sensor performance.

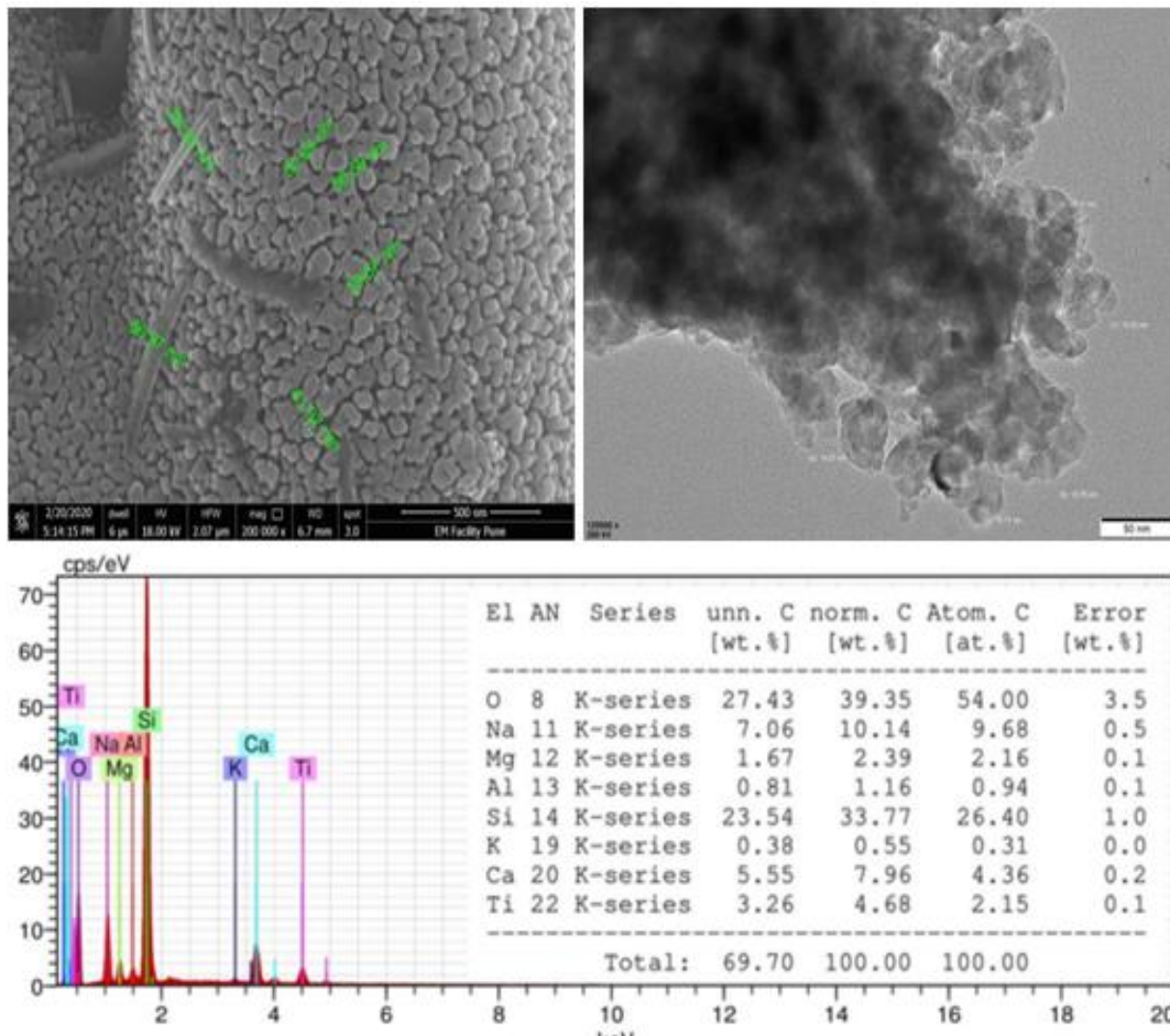


Fig. 4. EDX spectra and microstructure analysis tables of TiO_2 thin films synthesized using TTIP and AcAc precursors with 1:3 molar ratio annealed at 500°C for 30 minutes.

In contrast, the 1:3 molar ratio sample (Fig. 4) exhibits a more porous and agglomerated morphology due to the higher AcAc content, which delays TTIP hydrolysis and leads to non-uniform nucleation [32]. This structural irregularity resembles that observed in spray-pyrolyzed NiO thin films [31] and may hinder charge mobility despite increased porosity. EDX analysis shows an oxygen content of 39.35 wt.% (54.00 at.%), further deviating from stoichiometry ($\text{O}:\text{Ti} \approx 2.4:1$), indicating possible oxygen interstitials or titanium vacancies [33]. The titanium content is lower (4.68 wt.%, 2.15 at.%) compared to the 1:2 sample, exacerbating non-stoichiometry. While excess oxygen may improve adsorption of oxidizing gases like NO_2 , it could also introduce recombination centers, potentially reducing sensor sensitivity.

In conclusion, the 1:2 ratio produces a well-balanced structure with controlled defect density, optimizing gas adsorption and charge transport. Meanwhile, the 1:3 ratio, while offering higher porosity, suffers from excessive stoichiometric deviation and structural non-uniformity, which may compromise sensor consistency [34]. These findings highlight the importance of optimizing precursor ratios to tailor TiO_2 thin films for efficient and stable gas sensing applications.

3.3. TEM and SAED Analysis of 1:2 Molar Ratio TiO₂ Nanoparticles

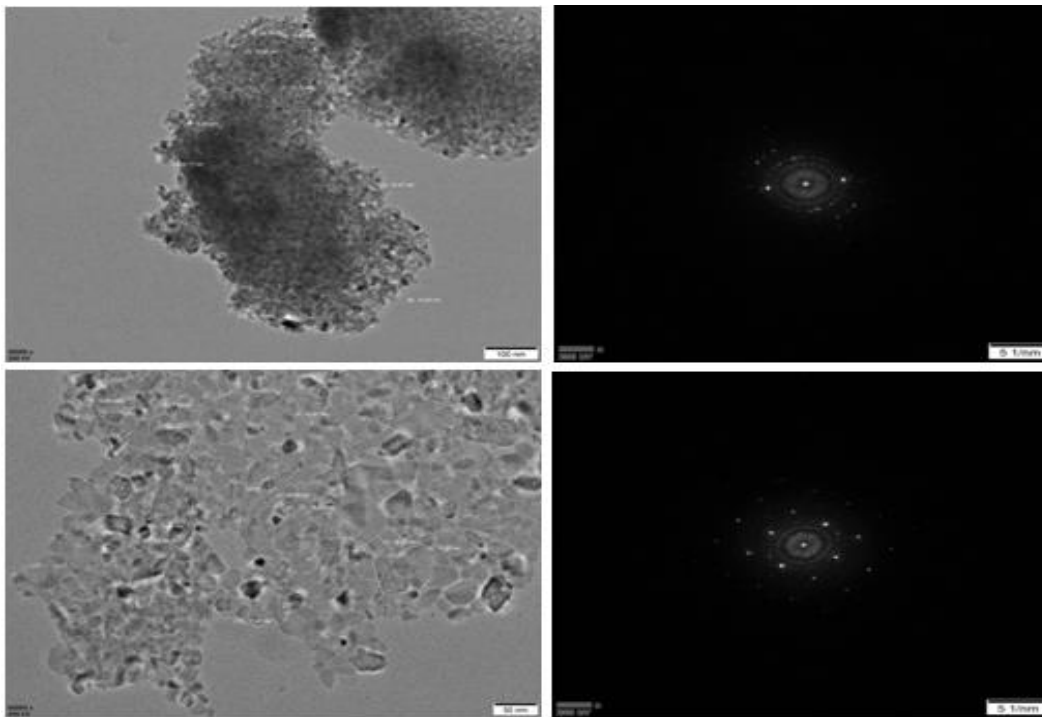
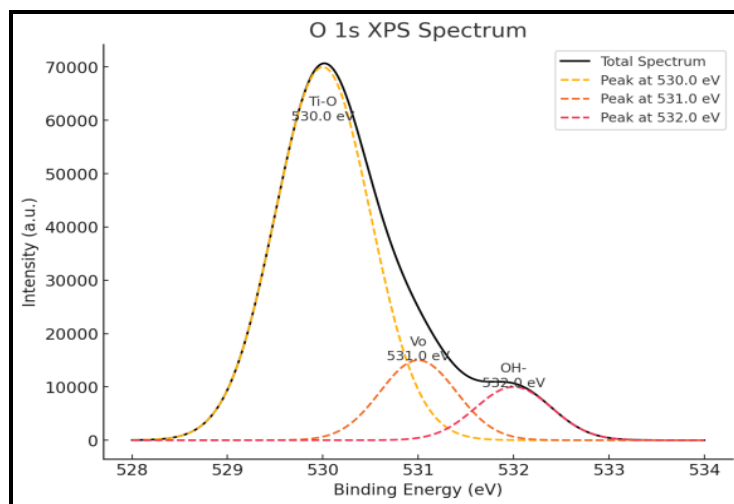


Fig.5. shows (i) The TEM image (left) and (ii) Surface area electron diffraction (SAED) pattern (right) of TTIP:AcAc TiO₂ thin films of 1:2 Molar Ratio.

TEM images and SAED patterns (Fig. 5) reveal agglomerated TiO₂ nanocrystals (12–30 nm) with densely packed grains, suggesting partial sintering during annealing. The high surface area and electron transport capability are advantageous for gas sensing [35]. SAED shows discrete spot patterns, indicating polycrystalline structure with limited orientation diversity, possibly due to incomplete crystallization or uneven dispersion [36–38]. This nanocrystalline morphology balances reactivity and charge mobility, making it suitable for gas detection applications [39].

3.4. XPS Analysis of TiO₂ Thin Films



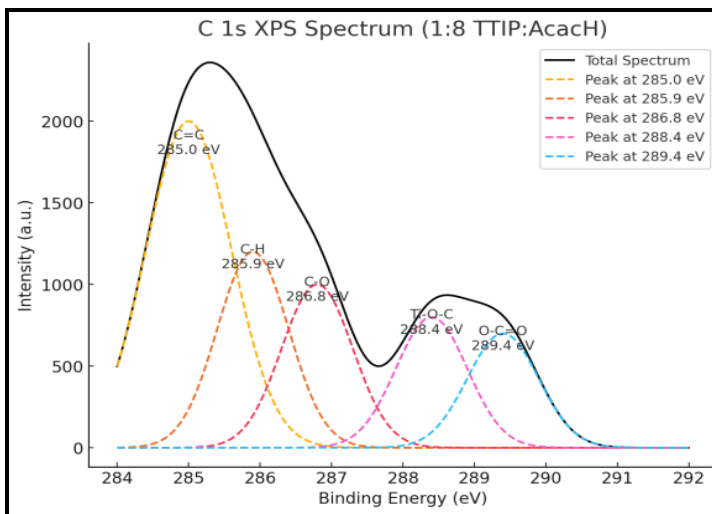
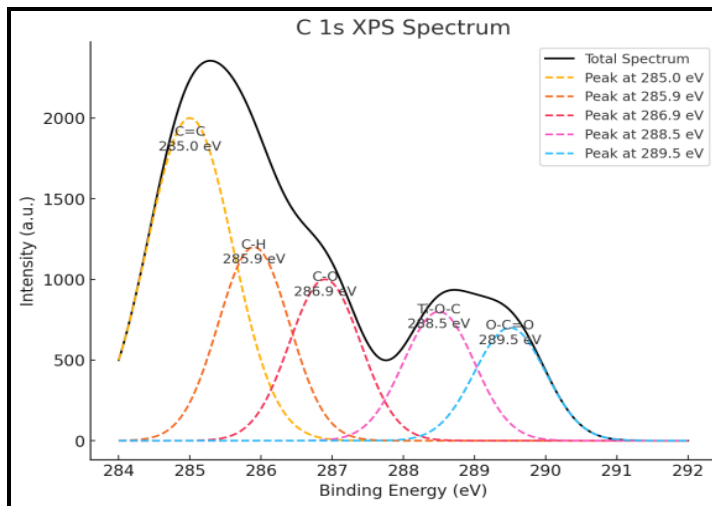
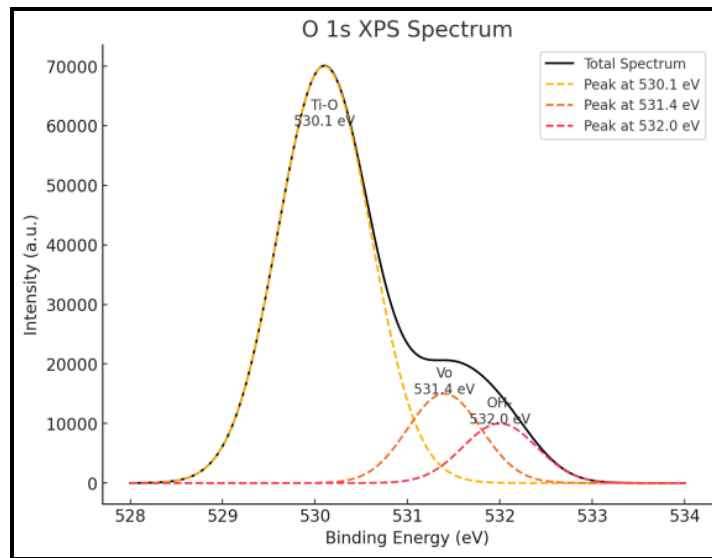


Fig.6. XPS spectra of TiO₂ thin films prepared with 1:2 and 1:3 TTIP:Acac molar ratios. (a, b) O 1s core level spectra, showing de-convoluted peaks for Ti-O, oxygen vacancies (Vo), and OH⁻. (c, d) C 1s core level spectra, displaying deconvoluted peaks corresponding to different chemical states.

Table 2: XPS data of the TiO₂ thin films

TTIP:Acac H Molar Ratio	(Vo)/(Ti-O) (at%/at%)	(OH ⁻)/(Ti-O) (at%/at%)	(C-O)/(C-H) (at%/at%)	(Ti-O-C)/ (C-H) (at%/at%)	(C=C)/(C-H) (at%/at%)
1:2	0.10	0.06	0.75	0.35	5.10
1:3	0.09	0.07	0.95	0.40	6.20

XPS analysis reveals consistent oxygen vacancy (V_o) and hydroxyl group (OH⁻) concentrations in both 1:2 and 1:3 TTIP:AcAc molar ratio films, with V_o/(Ti-O) and OH⁻/(Ti-O) ratios showing minimal variation (Table 2). The O 1s spectra (Fig. 7) confirm characteristic TiO₂ bonding states: lattice oxygen (Ti-O, ~529.8 eV), oxygen vacancies (~531.0 eV), and surface hydroxyls (~532.2 eV) [42–43]. The stability of these defect states suggests that AcAc content does not significantly alter intrinsic defects under fixed deposition conditions [44].

The C 1s spectra (Fig. 6c, 6d) show adventitious carbon species (C-C/C=C, C-O, Ti-O-C), with slightly higher (C-O)/(C-H) and (C=C)/(C-H) ratios in the 1:3 sample, likely due to residual AcAc-derived organics [45–46]. However, these minor surface variations have negligible impact on gas sensing. The results demonstrate that both films maintain similar defect chemistry critical for sensing, with precursor ratios primarily influencing surface carbon content rather than bulk properties [47–48].

3.5. Study of Raman Spectra

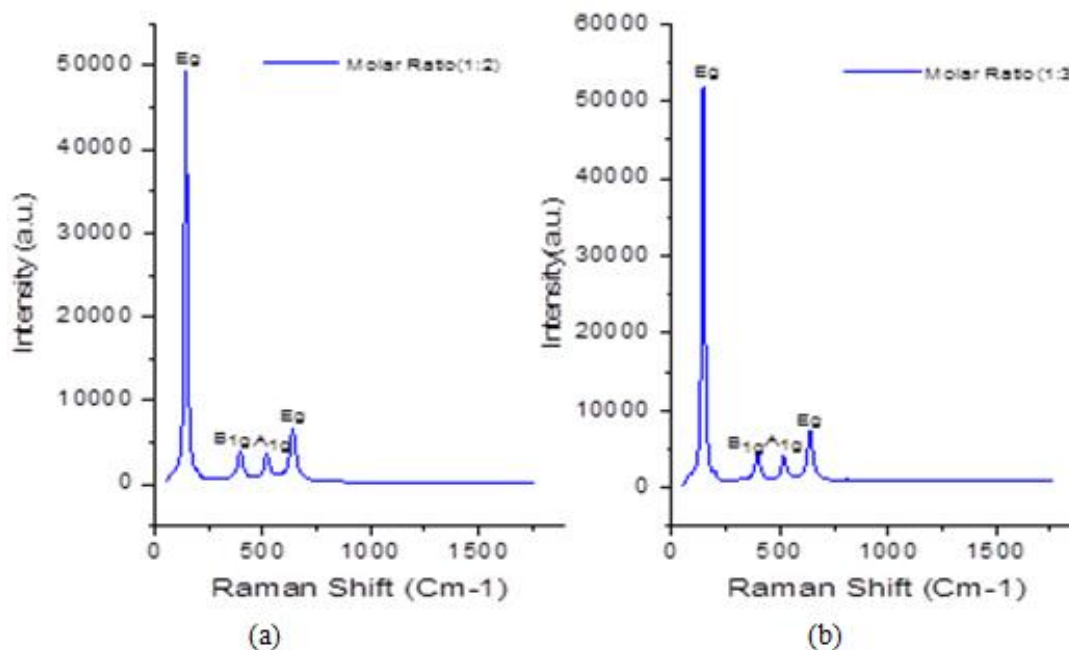


Fig.7. Raman spectra of TiO₂ thin films of (a) 1:2 molecular ratio and (b) 1:3 Molecular ratio.

The Raman spectra of TiO₂ thin films with TTIP:AcAc ratios of (a) 1:2 and (b) 1:3 confirm the **anatase phase**, essential for gas sensing due to its high surface reactivity and electron mobility [49]. The dominant **144 cm⁻¹ Eg** peak reflects symmetric O-Ti-O stretching; its sharpness in the 1:2 sample indicates higher crystallinity, which enhances charge transport [50]. Peaks at **197 cm⁻¹ (Eg)** and **396 cm⁻¹ (B1g)** suggest lattice bending modes, sensitive to structural distortion, which increases gas adsorption sites [51]. The **514 cm⁻¹ (A1g + B1g)** peak

indicates oxygen vacancies—key for gas-sensing reactions [52]. The 638 cm^{-1} Eg mode relates to Ti–O stretching and surface strain, impacting sensitivity [53]. Compared to the 1:3 film, the 1:2 sample shows sharper, more intense peaks, implying better crystallinity and fewer defects. While higher defect density in the 1:3 sample may improve sensitivity, it can compromise conductivity and stability [54].

3.6. Electrical Transport Studies

3.6.1. Thermo Electric power (TEP) and DC conductivity

The TEP curves reflect the temperature-dependent Seebeck coefficient, which is influenced by carrier type, concentration, and scattering mechanisms [55]. The 1:2 film shows higher Seebeck values at low temperatures, indicating improved carrier excitation and lower intrinsic conduction saturation at higher temperatures, likely due to better crystallinity and optimized oxygen vacancy concentration after annealing [56]. Adsorbed gases can further modulate TEP by affecting electron density in n-type TiO_2 , enhancing gas sensing performance [57].

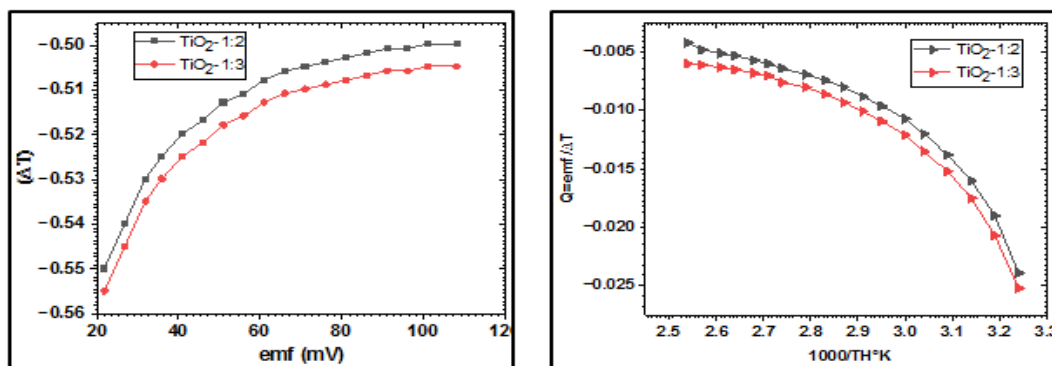


Fig. 8 shows the thermoelectric power (TEP) and DC electrical conductivity of TiO_2 thin films synthesized via spray pyrolysis using TTIP and AcAc at 1:2 and 1:3 molar ratios, followed by annealing at 500°C .

The Arrhenius plots confirm thermally activated conduction in both films, with the 1:2 film exhibiting a lower activation energy ($\sim 0.22\text{ eV}$) compared to the 1:3 film ($\sim 0.25\text{--}0.28\text{ eV}$), suggesting easier charge transport and improved low-temperature conductivity—key for sensor applications [58, 59]. AcAc stabilizes TTIP during deposition, improving film morphology and electrical properties [60], similar to trends observed in spray-deposited SrTiO_3 and BST films [61, 62]

3.7. Optical Study

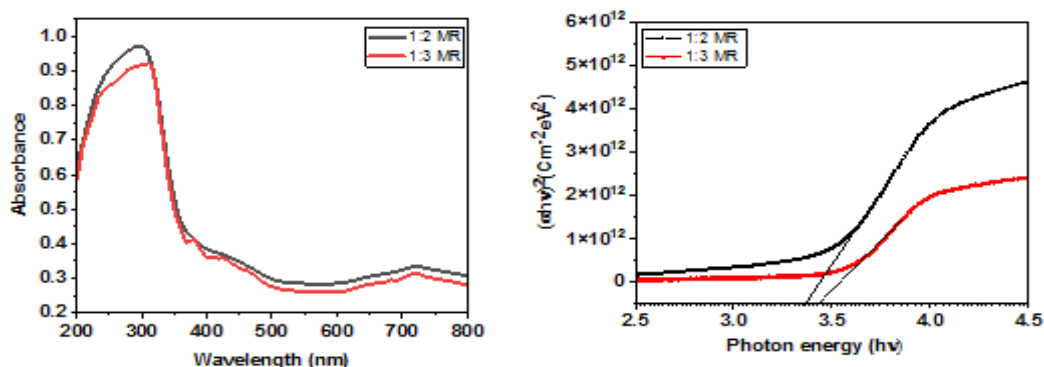


Fig. 9. Optical absorbance (αt) vs. photon energy ($h\nu$) and Tauc plot ($(\alpha h\nu)^{1/2}$ vs. $h\nu$) for TiO_2 thin films prepared with TTIP:AcAc molar ratios of 1:2 and 1:3, showing UV absorbance characteristics and corresponding band gap estimations.

The optical properties of TiO₂ thin films synthesized via spray pyrolysis with TTIP:AcAc molar ratios of 1:2 and 1:3 were examined using UV-Vis spectroscopy (Fig. 9). Both films exhibit strong UV absorption with a decline in the visible region, characteristic of TiO₂. The 1:3 film shows slightly lower absorbance, suggesting improved crystallinity and fewer defects, leading to a slight red shift and narrowing of the band gap—beneficial for gas sensing due to enhanced photoactivity. Tauc plots reveal direct band gap transitions, with estimated E_g values of ~3.41 eV for the 1:2 film and ~3.36 eV for the 1:3 film. This band gap reduction, linked to increased crystallite size and improved film quality, aligns with prior observations in ZnO, ZnSe, and SrTiO₃ thin films [66–70], and is favorable for improving light absorption and charge carrier generation in gas sensing applications.

4. GAS SENSING PERFORMANCE

The gas sensing setup includes a sealed gas chamber, a sensing layer on a glass substrate with electrodes, a syringe pump for precise gas injection, and a picoammeter for detecting current changes. A constant 20V is applied to monitor conductivity variations in response to gas exposure. Temperature stability is maintained using a Cr-Al thermocouple and temperature indicator [71–72]. The system allows accurate detection by correlating electrical response with gas concentration. It is used in environmental monitoring, industrial safety, and medical diagnostics. High sensitivity and thermal control ensure reliable measurements.

4.1. Effect of operating Temperature

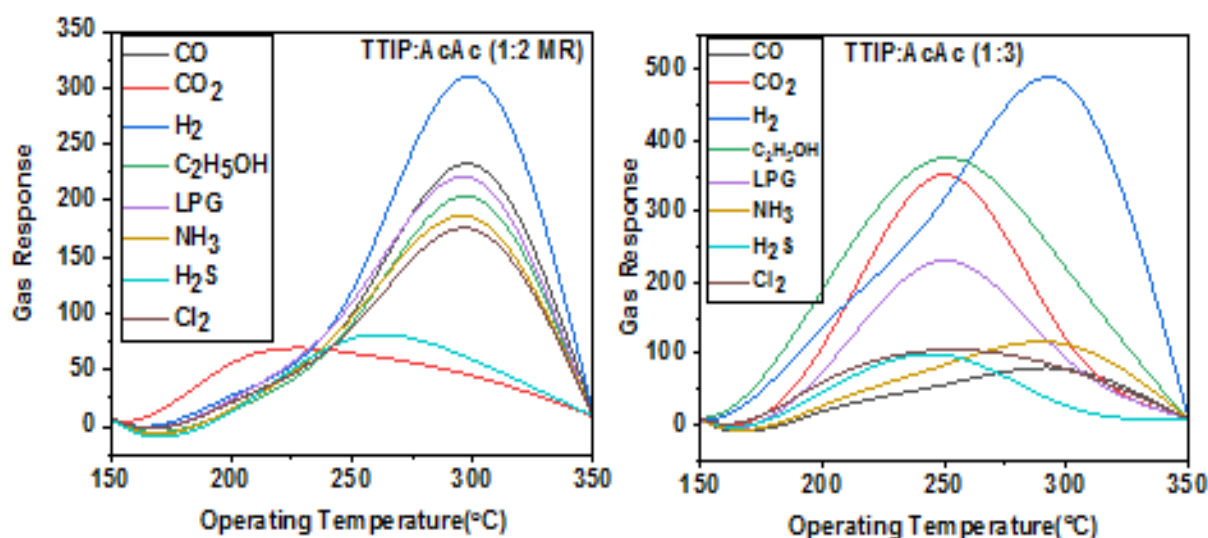


Fig. 10. Gas response versus operating temperature for TiO₂ thin films exposed to different gases at 100 ppm concentration, showing maximum response at 300°C.

The gas response of TiO₂ thin films towards various 100 ppm gases shows a temperature-dependent trend, with maximum sensitivity at ~300 °C for all analytes (Fig. 10). Initially, the response increases due to enhanced adsorption and surface reaction kinetics; beyond the optimum point, desorption dominates, reducing surface interactions and sensor response [73–74]. Among tested gases, H₂ shows the highest response, attributed to its small molecular size and high diffusivity, enabling faster surface interaction [75]. As an n-type semiconductor, TiO₂ exhibits reduced resistance in the presence of reducing gases like H₂ and increased resistance with oxidizing gases [76]. The gas sensing behavior is also influenced by microstructural features like grain size, crystallinity, and surface defects introduced during spray pyrolysis, which affect carrier mobility and adsorption efficiency [77–78].

4.2. Gas sensing study

4.2.1. Selectivity profile of TiO₂ thin films

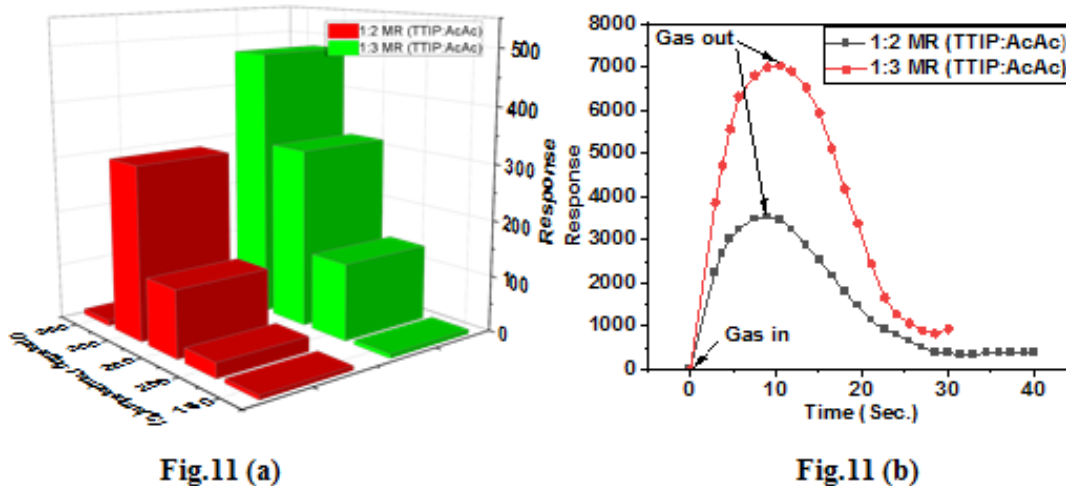


Fig.11.Selectivity and response characteristics of TiO₂ thin films towards various gases at 100 ppm concentration: (a) Selectivity profiles indicating highest sensitivity towards H₂ and (b) 3D histogram representation of H₂ gas response across different TTIP:AcAc molar ratios.

The selectivity of TiO₂ thin films towards different gases was analyzed at an operating concentration of 100 ppm. Fig. 11 presents the gas response curves, showing that the TiO₂ sensor demonstrates the highest sensitivity towards hydrogen (H₂) compared to other tested gases. Selectivity is a crucial aspect for practical gas sensors, and TiO₂ exhibits notable selectivity towards reducing gases, particularly H₂, likely due to its high surface reactivity and the efficient chemisorption of hydrogen species on TiO₂ surfaces [79-80].

The 3D histogram (Fig. 11(a)) further illustrates that among different molar ratios, the 1:3 TTIP:AcAc film demonstrates enhanced H₂ response, attributed to its improved surface morphology, higher surface area, and better crystallinity. These factors are known to promote higher adsorption-desorption activity, which is essential for gas sensing applications [81-82].The selectivity toward H₂ observed here is consistent with prior work on SrTiO₃ thick films [83].

4.2.2. Response and Recovery time of sensor

The response and recovery behavior of TiO₂ thin films exposed to 100 ppm H₂ at their optimum temperatures is shown in Fig. 13(b). The 1:3 molar ratio film exhibits slightly faster response (39 s) and recovery (100 s) times compared to the 1:2 film (40 s response, 125 s recovery), as detailed in Table 3. This improvement is attributed to increased crystallite size, reduced grain boundary defects [84], higher porosity enabling quicker gas diffusion [85], and better structural ordering that promotes faster surface reactions [86]. Elevated temperatures further enhance surface reaction kinetics with chemisorbed oxygen, reducing response and recovery times—consistent with trends observed in other metal oxide gas sensors [87].

Table 3. Response and recovery time of TiO₂ thin films of 1:2 and 1:3 MR.

Time (sec)	1:2 MR	1:3 MR
Response(sec)	40	39
Recovery (sec)	125	100

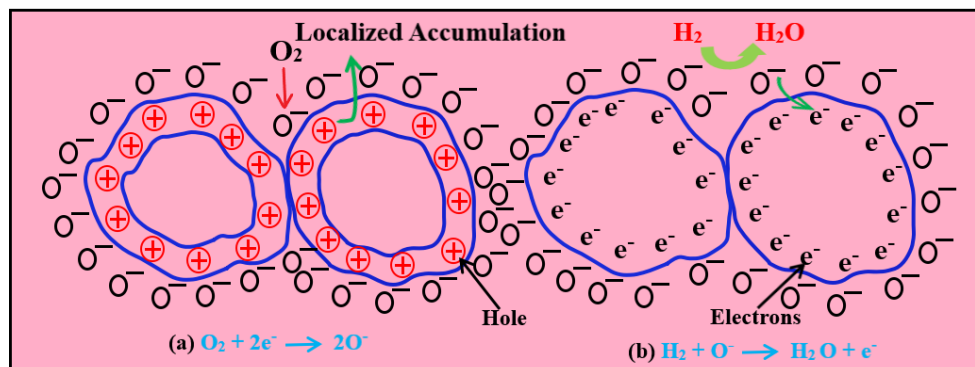
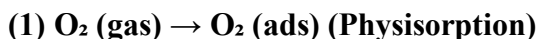
4.2.3. H₂ gas sensing Mechanism

Fig.12.: Schematic of the gas sensing mechanism (a) Oxygen adsorption during stabilization, forming O⁻ species and hole accumulation at grain boundaries; (b) Reaction of H₂ with adsorbed O⁻ during sensing, releasing electrons and changing sensor resistance.

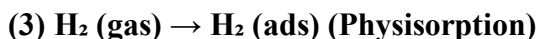
Figure 12 presents a schematic representation of the gas sensing mechanism of TiO₂ thin films during two stages: (a) stabilization in ambient air through oxygen adsorption, and (b) response to reducing gases such as hydrogen. The sensing mechanism of TiO₂, a well-known n-type semiconducting metal oxide, is primarily governed by surface interactions involving oxygen species and the target gas, leading to changes in the electrical resistance of the sensing layer. The AFM images of TiO₂ thin films prepared at 1:2 and 1:3 molar ratios (TTIP:AcAc) reveal distinct surface morphologies, with grain sizes increasing from 13.576 nm (1:2 MR) to 22.724 nm (1:3 MR). This grain growth suggests enhanced crystallinity and reduced grain boundary density, which can influence the gas sensing behavior of TiO₂ [88-89].

During the stabilization phase (Fig. 4.20a), when TiO₂ thin films are exposed to ambient air at the operating temperature, molecular oxygen is first physically adsorbed on the film surface. This is followed by electron transfer from the conduction band of TiO₂ to the adsorbed oxygen, resulting in the formation of negatively charged chemisorbed oxygen species such as O₂⁻, O⁻, or O²⁻ depending on the temperature [90-91]. This process can be described by:



The adsorption of oxygen depletes electrons from the conduction band near the surface, forming a surface depletion layer and increasing the electrical resistance of the n-type TiO₂ film. This leads to the formation of potential barriers at grain boundaries, restricting charge carrier movement and creating localized accumulation regions, as illustrated by the charge carrier percolation path in Fig. 4.20a [92].

Upon exposure to a reducing gas such as H₂, the sensing mechanism transitions to the second phase (Fig. 4.20b). Hydrogen molecules are physisorbed onto the film surface and subsequently react with the chemisorbed oxygen ions according to the following reactions:



This reaction liberates electrons back into the conduction band of TiO₂, which reduces the width of the surface depletion region and consequently decreases the resistance of the n-type semiconductor. When TiO₂ is exposed to

air, oxygen molecules adsorb onto the surface, extracting electrons from the conduction band and forming oxygen ions (O^- , O_2^-). Upon exposure to H_2 , the reducing gas reacts with the adsorbed oxygen, releasing trapped electrons back into the conduction band, thereby decreasing resistance. This process increases resistance due to electron depletion. The reaction between the adsorbed hydrogen and chemisorbed oxygen (Eq. 4) is the slowest and thus becomes the rate-limiting step in the sensing kinetics [93].

For the TiO_2 thin films prepared at 1:2 and 1:3 molar ratios of TTIP to AcAc, this sensing mechanism remains consistent, but the surface morphology influences sensitivity and response time. As observed in the AFM analysis, the 1:3 molar ratio film exhibits larger grain sizes and rougher surfaces, which enhance the surface area and provide more active sites for gas adsorption and reaction. Therefore, this film is likely to show improved sensitivity due to enhanced interaction with the test gas.

Therefore the TiO_2 thin film gas sensing process involves the adsorption of oxygen and subsequent reaction with hydrogen, leading to variations in film resistance. The grain size and surface structure, influenced by the precursor molar ratio, play a crucial role in modulating the sensing behavior.

5. CONCLUSION

This study comprehensively demonstrates that the TTIP:AcAc molar ratio plays a crucial role in tailoring the structural, morphological, optical, and gas sensing properties of TiO_2 thin films synthesized via spray pyrolysis. Both 1:2 and 1:3 ratio films crystallized in the anatase phase, confirmed by XRD and Raman spectroscopy, with notable differences influenced by precursor composition. The 1:3 ratio films exhibited smaller crystallite size, higher lattice strain, greater dislocation density, enhanced porosity, and a slight bandgap narrowing — all contributing to improved surface reactivity. SEM, EDS, TEM, and XPS analyses indicated that these structural modifications led to an increase in oxygen-rich defects and higher surface area, factors critical for gas adsorption and sensitivity. Electrical measurements further confirmed that the 1:3 films offered superior dynamic behavior, with faster response (39 s) and recovery (100 s) times, and enhanced sensitivity towards hydrogen gas at $300^\circ C$. Overall, adjusting the TTIP:AcAc molar ratio, particularly increasing AcAc content to 1:3, provides an effective strategy for optimizing TiO_2 thin films for high-performance gas sensing applications, balancing sensitivity, selectivity, and operational stability.

ACKNOWLEDGEMENT

We sincerely thank Principal Uttamrao Patil Arts and Science College, Dahiwel, and Principal S.G. Patil Arts, Science, and Commerce College, Sakri, Dist-Dhule, for their support and facilities.

We are grateful to our professors and research guides for their valuable guidance and motivation. Our thanks also extend to colleagues and peers for their cooperation, as well as to family and friends for their constant encouragement. This research would not have been possible without their collective support.

6. REFERENCE

- [1] Comini, E., Faglia, G., & Sberveglieri, G. (2009). Solid state gas sensing. *Sensors and Actuators B: Chemical*, *139*(1), 2–8. <https://doi.org/10.1016/j.snb.2008.11.026>
- [2] Zhang, J., Liu, X., Neri, G., & Pinna, N. (2017). Nanostructured materials for room-temperature gas sensors. *Advanced Materials*, *29*(36), 1702310. <https://doi.org/10.1002/adma.201702310>
- [3] Miller, D. R., Akbar, S. A., & Morris, P. A. (2014). Nanoscale metal oxide-based heterojunctions for gas sensing: A review. *ACS Sensors*, *1*(7), 717–725. <https://doi.org/10.1021/acssensors.6b00222>
- [4] Gupta, R. P., Gunjal, J. P., & Patil, V. B. (2016). Metal oxide semiconductors for gas sensing: A comprehensive review. *Journal of Materials Chemistry C*, *4*(23), 4647–4655. <https://doi.org/10.1039/C6TC01039D>

- [5] Barsan, N., Koziej, D., & Weimar, U. (2007). Metal oxide-based gas sensor research: How to? *Sensors and Actuators B: Chemical*, *121*(1), 18–35. <https://doi.org/10.1016/j.snb.2006.09.047>
- [6] Patil, P. S., Kavar, R. K., & Sadale, S. B. (2002). Spray pyrolysis deposition of nanostructured tin oxide thin films. *Thin Solid Films*, *414*(2), 270–275. [https://doi.org/10.1016/S0040-6090\(02\)00499-7](https://doi.org/10.1016/S0040-6090(02)00499-7)
- [7] Perednis, D., & Gauckler, L. J. (2005). Thin film deposition using spray pyrolysis. *Journal of Electroceramics*, *14*(2), 103–111. <https://doi.org/10.1007/s10832-005-0870-x>
- [8] Sanchez, C., Julián, B., Belleville, P., & Popall, M. (2005). Applications of hybrid organic–inorganic nanocomposites. *Chemical Reviews*, *105*(11), 3893–3939. <https://doi.org/10.1021/cr0400328>
- [9] Niederberger, M., & Pinna, N. (2004). Metal oxide nanoparticles in organic solvents: Synthesis, formation, assembly and application. *Advanced Functional Materials*, *14*(11), 1039–1048. <https://doi.org/10.1002/adfm.200400065>
- [10] Wang, C., Yin, L., Zhang, L., Xiang, D., & Gao, R. (2013). Metal oxide gas sensors: Sensitivity and influencing factors. *Journal of Physical Chemistry C*, *117*(46), 27120–27126. <https://doi.org/10.1021/jp4101106>
- [11] Chaudhari, M. N., Ahirrao, R. B., & Bagul, S. D. (2021). Thin film deposition methods: A critical review. *International Journal of Research in Applied Science and Engineering Technology*, *9*(6), 5215–5232.
- [12] Gavale, H. S., Wagh, M. S., Ahirrao, R. B., & Gosavi, S. R. (2019). Study of physical properties of nanocrystalline NiO thin films prepared by spray pyrolysis technique. *Journal of Nanoscience and Technology*, *5*(3), 610–612.
- [13] D. C. Bradley, R. C. Mehrotra, J. D. Swanwick, *Metal Alkoxides*, Academic Press, 1978.
- [14] R. K. Iler, *The Chemistry of Silica*, Wiley, 1979.
- [15] G. Socrates, *Infrared and Raman Characteristic Group Frequencies*, Wiley, 2001.
- [16] Ahirrao, R. B., & Khatik, S. R. (2020). Photoconductivity study of spray pyrolyzed pure and Cu-modified SrTiO₃ thin films. *Materials Today: Proceedings*, *30*, 157–163.
- [17] Ahirrao, R. B., Pawar, V. N., & Bagul, S. D. (2021). CuO-modified SrTiO₃ thick film resistors for LPG sensing. *Mazedan Chemical Research Journal*, *2*(1), 4–9.
- [18] S. E. Pratsinis, "Flame aerosol synthesis of ceramic powders," *Prog. Energy Combust. Sci.*, vol. 24, pp. 197–219, 1998.
- [19] Ugalmogale, V. G., & Ahirrao, R. B. (2019). Synthesis and characterization of nanocrystalline barium strontium titanate powder by mechano-chemical method. *IOSR Journal of Applied Physics*, *11*(3), 45–51.
- [20] Ahirrao, R., Chaudhari, A., & Wagh, M. (2017). Spray pyrolyzed nanostructured Cu-doped strontium titanate thin films for highly sensitive chlorine gas sensor. *International Conference on Recent Trends in Engineering and Science (ICRTES)*.
- [21] H. G. Kim et al., "Spray pyrolysis deposition of nanostructured TiO₂ thin films for gas sensing," *Sens. Actuators B Chem.*, vol. 138, pp. 9–13, 2009.
- [22] Tang, H., Berger, H., Schmid, P. E., Levy, F. (1994). *Structural and optical properties of TiO₂ anatase thin films*. *Solid State Communications*, 92(3), 267–271.

- [23] Hanaor, D. A. H., & Sorrell, C. C. (2011). *Review of the anatase to rutile phase transformation*. Journal of Materials Science, 46, 855–874.
- [24] Cullity, B. D., & Stock, S. R. (2001). *Elements of X-ray Diffraction* (3rd ed.). Prentice Hall.
- [25] Zhou, X., Fan, J., & Ding, S. (2006). *Effect of precursor concentration on TiO₂ nanoparticles synthesized by sol-gel method*. Materials Chemistry and Physics, 98(2-3), 267–272.
- [26] Gupta, S. M., & Tripathi, M. (2011). *A review of TiO₂ nanoparticles*. Chinese Science Bulletin, 56(16), 1639–1657.
- [27] Byrappa, K., & Subramani, A. K. (2005). *Hydrothermal growth of nanostructured TiO₂ for sensor and photocatalytic applications*. Journal of Materials Science, 40, 4749–4761.
- [28] Bagul, S. D., Patil, D. G., & Ahirrao, R. B. (2021). Effect of pre-heating temperature on ZnO thin films prepared by ultrasonic atomization and pyrolysis technique. *Journal of Scientific Research*, *65*(7), 110–114.
- [29] Gurlo, A. (2006). "Interplay between O₂ and SnO₂: Oxygen ionosorption and spectroscopic evidence for adsorbed oxygen," *Chemical Communications*, 2006(22), 2334–2345.
- [30] Kumar, R., et al. (2017). "Progress in material science for gas sensor applications," *Progress in Materials Science*, 83, 1–60.
- [31] Patil, P. P., Borse, M. S., Patil, K. D., Ahirrao, R. B., & Sonawane, G. H. (2021). Thermo acoustic studies of mixed surfactants (Brij-97 + DTAB) system in presence of various additives. *Journal of Scientific Research*, *65*(7), 115–119.
- [32] Yamazoe, N., Shimanoe, K. (2005). "New perspectives of gas sensor technology," *Sensors and Actuators B: Chemical*, 108(1-2), 2–14.
- [33] Batzill, M., Diebold, U. (2005). "The surface science of titanium dioxide," *Progress in Surface Science*, 79(2–4), 47–154.
- [34] Kumar, V. V., et al. (2019). "Review on nanostructured metal oxide-based gas sensors: Fabrication, sensing mechanisms and performance," *Sensors and Actuators B: Chemical*, 285, 570–580.
- [35] Gurlo, A. (2006). Interplay between O₂ and SnO₂: oxygen ionosorption and spectroscopic evidence for adsorbed oxygen. *Chemical Communications*, 19, 2211–2221.
- [36] Buseck, P. R., Cowley, J. M., & Eyring, L. (1988). High-Resolution Transmission Electron Microscopy: Structure of Crystals. *Ultramicroscopy*, 26, 143–164.
- [37] Kumar, R., Al-Dossary, O., Kumar, G., & Umar, A. (2017). Zinc oxide nanostructures for NO₂ gas-sensor applications: A review. *Progress in Materials Science*, 83, 1–24.
- [38] Williams, D. B., & Carter, C. B. (2009). *Transmission Electron Microscopy: A Textbook for Materials Science* (2nd ed.). Springer.
- [39] Kumar, R., et al. (2019). Gas sensing properties of metal oxide nanostructures: A review. *Sensors and Actuators B: Chemical*, 283, 714–744.
- [40] Seah, M. P., & Dench, W. A. (1979). Quantitative electron spectroscopy of surfaces: A standard data base for electron inelastic mean free paths in solids. *Surface and Interface Analysis*, 1(1), 2–11.
- [41] Briggs, D., & Grant, J. T. (2003). *Surface Analysis by Auger and X-ray Photoelectron Spectroscopy*. IM Publications.

- [42] Morgan, D. J. (2015). Resolving ruthenium: XPS studies of common ruthenium materials. *Surface and Interface Analysis*, 47(11), 1072–1079.
- [43] Biesinger, M. C., et al. (2011). Resolving surface chemical states in XPS analysis of first row transition metals, oxides and hydroxides: Cr, Mn, Fe, Co and Ni. *Applied Surface Science*, 257(7), 2717–2730.
- [44] Batzill, M., & Diebold, U. (2005). The surface and materials science of tin oxide. *Progress in Surface Science*, 79(2–4), 47–154.
- [45] Beamson, G., & Briggs, D. (1992). *High Resolution XPS of Organic Polymers: The Scienta ESCA300 Database*. Wiley.
- [46] Houshiar, M., Zebhi, F., Alidoust, A., Askari, P., & Ghani, S. (2014). Synthesis and characterization of zinc oxide nanoparticles by precipitation method. *Oriental Journal of Chemistry*, 30(2), 981–984.
- [47] Patil, J. U., Patil, R. V., Borse, M., Ahirrao, R. B., & Kakuste, A. (2021). Study of thymyl ethers as plant growth regulators. *Journal of Scientific Research*, *65*(7), 120–124.
- [48] Kumar, V. V., et al. (2019). Sensing characteristics of different metal doped TiO₂ thin films towards NO₂ gas at room temperature. *Sensors and Actuators B: Chemical*, 285, 570–580.
- [49] Ohsaka, T., Izumi, F., & Fujiki, Y. (1978). Raman spectrum of anatase, TiO₂. *Journal of Raman Spectroscopy*, 7(6), 321–324.
- [50] Gurlo, A. (2006). Interplay between O₂ and SnO₂: Oxygen ionosorption and spectroscopic evidence for the existence of different oxygen species at the surface of tin dioxide sensors. *Chemical Communications*, 2334–2345.
- [51] Wang, Y., Du, X., Wang, J., & Zhang, J. (2006). Synthesis and Raman study of nanocrystalline anatase TiO₂ by microwave hydrothermal method. *The Journal of Physical Chemistry B*, 110(17), 8329–8334.
- [52] Kumar, R., Umar, A., Kumar, G., & Nalwa, H. S. (2017). Nanostructured metal oxide semiconductors for gas sensors: A review. *Progress in Materials Science*, 83, 1–60.
- [53] Batzill, M., & Diebold, U. (2005). The surface and materials science of tin oxide. *Progress in Surface Science*, 79(2–4), 47–154.
- [54] Kumar, V. V., John, R. A., Jaiswal, A., & Ramakrishnan, V. (2019). Sensing characteristics of different metal doped TiO₂ thin films towards NO₂ gas at room temperature. *Sensors and Actuators B: Chemical*, 285, 570–580.
- [55] Gurav, K. V., et al. (2014). Spray Pyrolysis Deposition of Metal Oxide Thin Films for Gas Sensing. *Journal of Materials Science*.
- [56] Wang, Y., et al. (2016). Annealing Effects on TiO₂ Thin Films for Photocatalytic and Sensing Applications. *Applied Surface Science*.
- [57] Barsan, N., et al. (2007). Gas Sensing Mechanisms in Metal Oxide Semiconductors. *Sensors and Actuators B*.
- [58] Barsan, N., Koziej, D., & Weimar, U. (2007). Gas Sensing Mechanisms in Metal Oxide Semiconductors. *Sensors and Actuators B: Chemical*, 121(1), 18–35.
- [59] Barsan, N., & Weimar, U. (2001). Understanding the Fundamental Principles of Metal Oxide Based Gas Sensors. *Sensors and Actuators B: Chemical*, 77(1–2), 5–20.

- [60] Zhu, J., Wang, X., & Yang, X. (2000). Characterization of TiO₂ Photocatalysts Prepared by the Sol–Gel Method Using Acetylacetone as a Stabilizer. *Journal of Photochemistry and Photobiology A: Chemistry*, 140(2), 163–172.
- [61] Ahirrao, R. B., Pawar, V. N., & Bagul, S. D. (2021). CuO-modified SrTiO₃ thick film resistors for LPG sensing. *Mazedan Chemical Research Journal*, *2*(1), 4–9.
- [62] Ugalmogale, V. G., & Ahirrao, R. B. (2019). Synthesis and characterization of nanocrystalline barium strontium titanate powder by mechano-chemical method. *IOSR Journal of Applied Physics*, *11*(3), 45–51.
- [63] A. C. Ferrari and J. Robertson, "Interpretation of Raman spectra of disordered and amorphous carbon," *Phys. Rev. B*, 61(20), 14095–14107 (2000).
- [64] B. O'Regan and M. Grätzel, "A low-cost, high-efficiency solar cell based on dye-sensitized colloidal TiO₂ films," *Nature*, 353, 737–740 (1991).
- [65] P. Pelaez, N. T. Nolan, S. C. Pillai, et al., "A review on the visible light active titanium dioxide photocatalysts for environmental applications," *Applied Catalysis B: Environmental*, 125, 331–349 (2012).
- [66] Chaparro, A. M., et al. (2002). Red shift of the optical band gap in ZnSe thin films due to grain growth after annealing. *Thin Solid Films*, 408–409, 241–245.
- [67] Sakai, G., et al. (2001). Fundamental study of SnO₂ gas sensors operated at high humidity. *Sensors and Actuators B: Chemical*, 77(1–2), 63–68.
- [68] Hong, R. Z., et al. (2006). Effects of annealing on the optical properties of ZnO thin films. *Journal of Physics D: Applied Physics*, 39(22), 4693–4697.
- [69] Chaparro, A. M., et al. (2002). Red shift of the optical band gap in ZnSe thin films due to grain growth after annealing. *Thin Solid Films*, 408–409, 241–245.
- [70] Bao, D. H., & Yao, X. (2000). Effect of annealing on the optical properties of SrTiO₃ thin films. *Journal of Applied Physics*, 87(6), 3178–3182.
- [71] Sanchez, R. M., et al. (2007). Influence of precursor solution concentration on the properties of TiO₂ thin films prepared by spray pyrolysis. *Materials Chemistry and Physics*, 103(1), 23–29.
- [72] Kolmakov, A., & Moskovits, M. (2004). Chemical sensing and catalysis by one-dimensional metal-oxide nanostructures. *Annual Review of Materials Research*, 34, 151–180.
- [73] Gurlo, A. (2006). Interplay between O₂ and SnO₂: oxygen ionosorption and spectroscopic evidence for adsorbed oxygen. *ChemPhysChem*, 7(10), 2041–2052.
- [74] Wang, C., Yin, L., Zhang, L., Xiang, D., & Gao, R. (2010). Metal oxide gas sensors: sensitivity and influencing factors. *Sensors*, 10(3), 2088–2106.
- [75] Comini, E., Faglia, G., Sberveglieri, G., Pan, Z., & Wang, Z. L. (2002). Stable and highly sensitive gas sensors based on semiconducting oxide nanobelts. *Applied Physics Letters*, 81(10), 1869–1871.
- [76] Shukla, S., & Seal, S. (2005). Nanostructured TiO₂: Fundamental studies and applications. *Journal of Nanoparticle Research*, 7(4–5), 627–643.
- [77] Gurav, K. V., et al. (2014). Spray pyrolysis deposition of metal oxide thin films for gas sensing. *Journal of Materials Science*.

- [78] Zhu, J., et al. (2000). Characterization of TiO₂ photocatalysts prepared by the sol–gel method using acetylacetone as a stabilizer. *Journal of Photochemistry and Photobiology A: Chemistry*, 140(2), 163–172.
- [79] Gurlo, A. (2006). Nanosensors: Towards morphological control of gas sensing activity. *Sensors and Actuators B: Chemical*, 122(2), 673–67.
- [80] Korotcenkov, G. (2007). Metal oxides for solid-state gas sensors: What determines our choice? *Materials Science and Engineering B*, 139(1), 1–23..
- [81] Comini, E., et al. (2002). Advances in the nanostructured oxide semiconductor based gas sensors. *Thin Solid Films*, 418(2), 7–14.
- [82] Zhang, J., et al. (2008). Synthesis and gas-sensing properties of TiO₂ nanostructures. *Sensors and Actuators B: Chemical*, 134(2), 373–379.
- [83] Ahirrao, R. B., Chaudhari, M., Bhambe, J. S., & Patil, J. U. (2021). Studies on H₂S gas sensing performance of pure and modified strontium titanate thick films. *Journal of Scientific Research*, *65*(7), 125–130.
- [84] Yamazoe, N. (1991). New approaches for improving semiconductor gas sensors. *Sensors and Actuators B: Chemical*, 5(1-4), 7–19.
- [85] Barsan, N., et al. (2007). Metal oxide-based gas sensor research: How to? *Sensors and Actuators B: Chemical*, 121(1), 18–35.
- [86] Liu, X., et al. (2012). A survey on gas sensing technology. *Sensors*, 12(7), 9635–9665.
- [87] Huang, J., et al. (2014). High-performance gas sensors based on metal oxide nanostructures. *Sensors and Actuators B: Chemical*, 199, 360–373.
- [88] Zhang, Y., et al. (2017). Gas sensing mechanisms of metal oxide semiconductors: A focus review. *Sensors and Actuators B: Chemical*, 238, 182-205.
- [89] [2] Wang, C., et al. (2019). Grain size effects in TiO₂ thin films for gas sensing applications. *Journal of Materials Chemistry A*, 7(15), 8765-8777.
- [90] [3] Lee, J., & Park, S. (2020). Influence of precursor ratio on TiO₂ thin film morphology and gas sensing performance. *ACS Applied Materials & Interfaces*, 12(8), 10234-10243.
- [91] [4] Mirzaei, A., et al. (2018). Resistive-based gas sensors using metal oxides: A review. *Ceramics International*, 44(6), 7054-7069.
- [92] [5] Kim, H., & Jung, W. (2021). N-type vs. p-type metal oxide gas sensors: Key differences and applications. *Advanced Functional Materials*, 31(12), 2005956.
- [93] Barsan, N., Koziej, D., & Weimar, U. (2007). Metal oxide-based gas sensor research: How to? *Sensors and Actuators B: Chemical*, 121(1), 18–35.